

# Low cost spinner developed for deposition of thin films used in OLED devices

## Spinner de baixo custo desenvolvido para deposição de filmes finos usados em dispositivos OLEDs

Emerson Roberto Santos<sup>1,2</sup>, Christine Miwa Takahashi<sup>2</sup>, Herick Garcia Takimoto<sup>1</sup>, Satoru Yoshida<sup>1</sup>, Mariane Tsubaki Oide<sup>1</sup>, Elvo Calixto Burini Júnior<sup>3</sup>, Roberto Koji Onmori<sup>4</sup>, Wang Shu Hui<sup>1</sup>

### ABSTRACT

This work aims the development of a compact spinner to be used inside the glove-box chamber to deposition of polymeric thin films used in the build of OLED devices. Initially, ten fans extracted of microcomputers were tested with commercial multi-voltage power supply. Four fans were selected based on the standard deviation of speed. A variable power supply was also built in order to get a more detailed response in terms of electrical current and speed in function of applied voltage. The fan that showed less variation of speed with applied voltage was selected for deposition tests using polymeric photoresist solution on the ITO (indium tin oxide) coated glass. This polymer was deposited by spin-coating at different speeds: 1000, 2000, 3000 and 4000 rpm and dried for the thicknesses measurement revealing good uniformity. Finally, three OLED devices were assembled with 2000 and 3000 rpm and the layers were dried under the same conditions. In the structure of the devices were used the materials deposited layer-by-layer: glass/ITO/PEDOT: PSS/Polyfluorene (PFpf)/Al. The OLED devices revealed blue light electroluminescence. The I-V curves showed better performance for OLED devices mounted at 2000 rpm with higher current density and similar appearance to the diode curve.

**Keywords:** Spinner, OLED, Current density, Electroluminescence.

### RESUMO

Este trabalho objetiva desenvolver um spinner compacto para utilização no interior de uma câmara glove box para deposição de filmes finos poliméricos para a montagem de dispositivos OLEDs. Inicialmente, dez ventoinhas foram extraídas de microcomputadores e testadas com fonte de alimentação comercial com multi-tensão. Foram selecionadas quatro ventoinhas com base no desvio padrão de velocidade. Uma fonte de energia variável foi montada para obter uma resposta mais detalhada em termos de corrente elétrica e velocidade em função da tensão aplicada. A ventoinha que apresentou menor variação na velocidade com a tensão aplicada foi selecionada para testes de deposição usando solução polimérica de fotorresiste sobre filmes de ITO (óxido de índio e estanho depositado sobre vidro). Este polímero foi depositado por spin-coating em diferentes velocidades: 1000, 2000, 3000 e 4000 rpm e seco para a medição de espessuras, revelando boa uniformidade. Três OLEDs foram montados em 2000 e 3000 rpm e as camadas foram secas sob as mesmas condições. Na estrutura dos dispositivos foram usados os materiais depositados camada-por-camada: vidro/ITO/PEDOT:PSS/Polyfluorene(PFpf)/Al. Os OLEDs revelaram eletroluminescência azul. As curvas I-V mostraram melhor desempenho para os OLEDs montados em 2000 rpm com mais elevada densidade de corrente e aparência similar à curva de diodo.

**Palavras-chave:** Spinner, OLED, Densidade de corrente, Eletroluminescência.

<sup>1</sup>Universidade de São Paulo – Escola Politécnica – Departamento de Engenharia Metalúrgica e de Materiais – São Paulo/SP – Brazil.

<sup>2</sup>Faculdade de Tecnologia de São Paulo – iCenter – Departamento de Sistemas Eletrônicos – São Paulo/SP – Brazil.

<sup>3</sup>Universidade de São Paulo – Instituto de Energia e Ambiente – São Paulo/SP – Brazil.

<sup>4</sup>Universidade de São Paulo – Escola Politécnica – Departamento de Engenharia Elétrica – São Paulo/SP – Brazil.

**Correspondence author:** Emerson Roberto Santos | Universidade de São Paulo – Escola Politécnica – Departamento de Engenharia Metalúrgica e de Materiais | Cidade Universitária | CEP 05.508-900 – São Paulo/SP – Brazil | E-mail: emmowalker@yahoo.com.br

**Received:** Jul. 21, 2017 | **Approved:** Apr. 17, 2018

## INTRODUCTION

OLED (Organic Light Emitting Diode) has been a promising optoelectronic device<sup>1,2</sup>. It differs from incandescent bulb lamp, which has a filament that generates luminescence<sup>3</sup>. Monochromatic OLEDs have been usually associated to applications that require less intense illumination<sup>4,6</sup>. Figure 1a shows a commercial monochromatic OLED with circular geometry and diameter of 76 mm (with red light emission) and Fig. 1b monochromatic OLED with rectangle geometry of 115 × 35 mm (with white emission), both supplied by Osram Company (Germany).

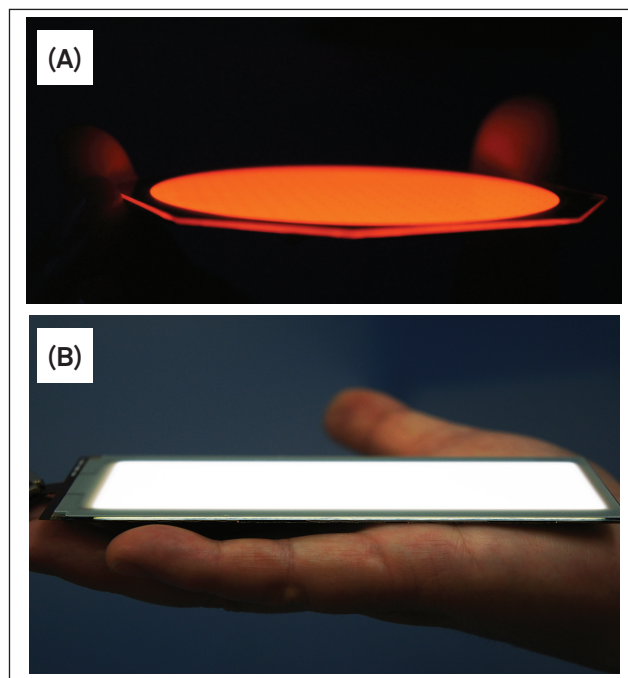


**Figure 1:** Commercial monochromatic OLED devices with: (A) circular active area and (B) rectangular active area.

The biggest challenge for the OLED industry has been to increment the efficiency and lifetime of these devices in order to compete with the conventional LEDs and this aspiration has urged the technological research<sup>7,8</sup>. In laboratory, the OLED assembling process has been carried out in a glove-box system with controlled humidity and inert atmosphere to reduce these problems<sup>9,10</sup>. OLED devices have polymeric-organic thin films sandwiched between inorganic electrodes the deposition of these organic materials have been carried out by spin coating method with commercial spinners<sup>11-13</sup>. The thickness and composition of the active polymeric-organic layer are very important because the light emission depends on the electrical current that flows through these layers.

As a matter of fact, electron and hole mobilities are changeable, depending on the material and morphology, although of utmost importance as a non-balanced number jeopardizes the charge recombination reducing the light emission and increasing the energy consumption<sup>14,15</sup>.

Commercial spinners have a motor, where the shaft is connected to a plain support (named as chuck) with small holes and bordered by a rubber ring for substrate fixation via vacuum<sup>16</sup>.

These equipments are expensive, robust and require connection to a vacuum pump to hold the sample during the rotation process<sup>17</sup>.

As the deposition of polymeric-organic thin film needs to be carried out in a glove-box, frequently, the size and connections of a commercial spinner need a customized glove-box with a large chamber. For this motive, in this work is proposed the assembly of a spinner with: compact size, low cost, easy method operation to assembly of thin films with good uniformity of the thicknesses as obtained by commercial spinners.

In 1958, Emslie et al. described the behavior of a viscous liquid on a rotating disk through hydrodynamic equations<sup>18</sup>. They reported that the final thickness of the fluid did not depend on the initial conditions of the fluid (before rotation) and the film thickness is determined by the solution dispersion after the beginning of rotation. Later, in 1978, Meyerhöfer reported that the dispersion caused by centrifugal force was mostly responsible for the thickness of the resultant film, nevertheless from a certain moment the film thickness was determined mainly by solvent evaporation<sup>19</sup>.

The spin coating has some stages: the solution is deposited on the blade, the blade is accelerated until the stabilization of the adjusted rotation resulting in a uniform speed and finally, the solution ceases to be expelled by centrifugal force and the thickness control is accomplished only by solvent evaporation<sup>20</sup>.

Figure 2 shows the complete spin coating process.

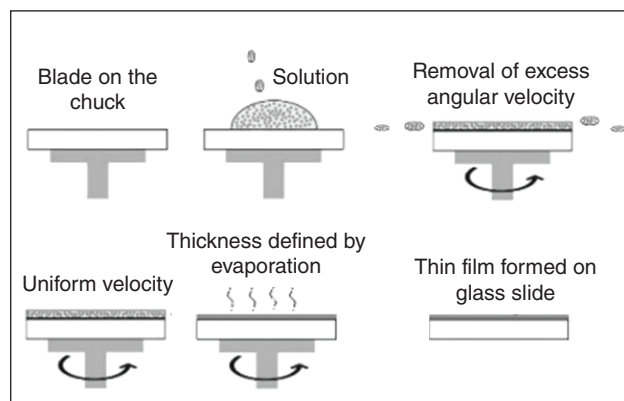


**Figure 2:** Formation of polymeric thin films by spin coating technique.

In summary, the final thickness of layer (that can be measured by various techniques as: profilometer, ellipsometry or AFM – atomic force microscopy of film depending on the order of magnitude) is influenced by various factors as: concentration of the material in the solution, initial speed of rotation, solvent evaporation rate, solution viscosity, vapor pressure and relative humidity. For these reasons, a meticulous analysis on the rotation behavior of the spinner mounted in this work should be performed.

## EXPERIMENTAL

### Analyses of the Fans

The spinner assembly started using ten fans of two sizes taken from obsolete microcomputers, three models of  $12.0 \times 12.0$  cm size and seven models of  $8.0 \times 8.0$  cm size. First the propeller blades were removed leaving only the shaft that will serve as the sample support (named as chuck). Each fan was identified by a letter, from A to Q. Table 1 shows manufacturer, electrical characteristic and size.

**Table 1:** Identification and specifications of the fans tested.

Identification fan	Manufacturer	Electrical characteristic	Size (cm)
A	ADDA Corporation (AD1212MS-A73GL)	12 VDC/ 0.34 A	12 × 12
B	ADDA Corporation (AD1212MS-A73GL)	12 VDC/ 0.34 A	12 × 12
C	New Flow (8025-S)	12 VDC/ 0.18 A	8 × 8
D	New Flow (8025-S)	12 VDC/ 0.18 A	8 × 8
E	Powersonic (PS-8025HS)	12 VDC/ 0.16 A	8 × 8
G	S8025M	12 VDC/ 0.15 A	8 × 8
H	KC8020H	12 VDC/ 0.18 A	8 × 8
I	Fukuryo(FM802512M)	12 VDC/ 0.15 A	8 × 8
J	Yuh Jonq (E149480)	12 VDC/ 0.13 A	8 × 8
Q	XT (Axial Fan)	12 VDC/ 0.28 A	12 × 12
P	ADDA	12 VDC/ 0.24 A	8 × 8

In this early stage a commercial power supply AD-1000 model, 18 W and 1000 mA was used. It can select different nominal output voltages: 1.5, 3.0, 4.5, 6.0, 7.5, 9.0 and 12.0 volts.

Measurements of voltage, electrical current and speed of rotation were taken for each position for all fans. The better fans present the lowest variation of speed at a given voltage. A multimeter manufactured by Minipa, ET- 1001 model was connected in parallel with the fan to measure the voltage, while another multimeter, ET-2082A model (Minipa) was connected in serial with the fan to measure the electrical current. For measurement of the rotation speed, a tachometer, MDT-2238A model (Minipa) set in photo-digital mode was used. This tachometer emits a light signal (red laser) that is reflected by a silver tape fixed on the fan shaft. Figure 3 shows the layout used for the speed and electrical measurements.

### Variable Power Supply Assembly

A variable power supply was built with a 15 V + 15 V center tapped transformer (maximum electrical current of 1.5 A). A fuze was connected to the transformer to avoid damages due to any voltage oscillation. To rectify the alternating current, two 1N4007 diodes were used and a 4,700  $\mu$ F and 50 V capacitor was used to reduce the ripple effect. For the voltage divider an LM317 IC was connected the 10 K potentiometer that allows the desired voltage setting. This variable power supply provides from 1.25 to 15 V, but 12 V was used due to the electrical specifications of the fans.

All electronic components and materials used to assemble the variable power supply are described on Table 2.

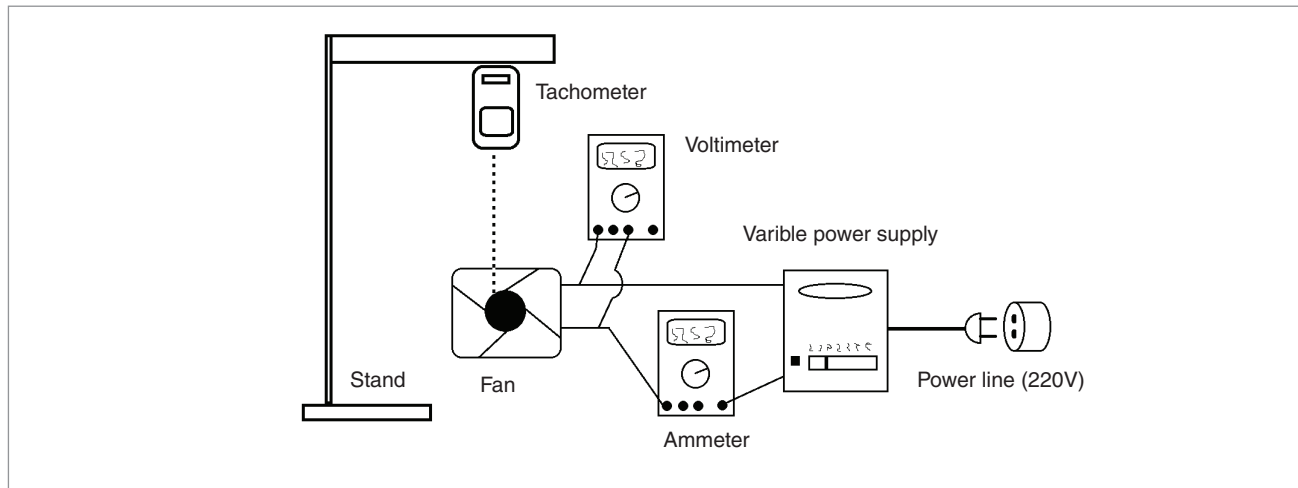


**Figure 3:** Layout showing the power supply and fan connected to measuring equipments.

**Table 2:** Materials used in the variable power supply prototype.

Power supply	Voltage regulator	Components
1 fuze and fuze holder 1 transformer (15 V + 15 V / 1.5 A) 2 1N4007 diodes 1 electrolytic capacitor (4700 $\mu$ F 50 V) wires and plugs	1 LM317 IC 1 heatsink 1 potentiometer B10K 2 1N4007 diodes 1 capacitor (10 $\mu$ F 100 V) 1 resistor 220 ohms	1 protoboard 10 borns jumpers screws wires for connection

## Electrical Circuit and Assembly of Spinner Apparatus

A printed circuit board (Fig. 4) was designed (with geometry of  $12.0 \times 7.0$  cm) using Proteus Ares software and drawn with a permanent ink pen on the cooper face of a phenolite board.

After drying the ink, the exposed areas were corroded with iron (III) chloride. Then the board was washed, dried and little holes were made with a mini drill, manufactured by Tozz Company for electronic components welding. The complete electrical circuit (with size  $12.0 \times 7.0$  cm) was placed within a plastic box; the on-off switch button and the speed of rotation control were adapted.

The chosen fan was screwed inside the bottom to prevent solution splashing during the rotation.

A double sided tape was used to fix the substrate to the motor shaft (used as chuck). Figure 5 shows the complete spinner apparatus.

### Assembly of OLED Devices

The OLED devices were prepared using ITO (indium tin oxide) of  $13 \Omega/\square$  deposited on glass substrates (manufactured by Diamond Coatings Limited) in geometry of  $2.5 \times 2.5$  cm. The substrates were cleaned with common detergent and running water to eliminate micro particles, immersed in the isopropyl alcohol and after in acetone, both by 30 min using ultrasonic bath<sup>21</sup>. To complement the cleaning process was used also a UV-Ozone apparatus to irradiation of ITO surfaces by 20 min<sup>22</sup>.

This process eliminates contaminants on the film and also contributes to a better spreading of the polymer.

The PEDOT:PSS [poly(3,4-ethylenedioxythiophene):poly-styrenesulfonate] (supplied by Sigma-Aldrich) thin film was deposited using different speeds with 2000 and 3000 rpm.

These films were dried at  $50^\circ\text{C}$  for 5 min. The emissive material with poly[(1,4-phenylene-2-fluor)-2,7-(9,9-dioctyl-fluorene)] (polyfluorene or PFpf) synthesized in laboratory was diluted in chloroform at 10 mg/mL, spin coated onto PEDOT:PSS film and dried at same condition previously used<sup>23</sup>. Finally, aluminium was thermally evaporated on the polyfluorene form the cathode. Organic thin film was measured by profilemeter with equipment of Veeco, model Dektak 6M with three measurements.

Three OLED (each device with its respective anode and cathode) were obtained at the same time on each blade. The samples were encapsulated in the glove box under nitrogen gas using glass with geometry of  $1.7 \times 1.7$  cm (covering all devices at the same time) and rubberized tape (manufactured by 3M, model VHB) at the edges<sup>24</sup>. Figure 6 shows the structure of OLEDs assembled.

A source meter manufactured by Keithley, model 2400 connected by Labtracer 2.0 software set as diode was used for the electrical characterization of OLED devices. Figure 6 shows the structure of OLED devices assembled. During the experiments the voltage was applied to obtain the respective electrical current.

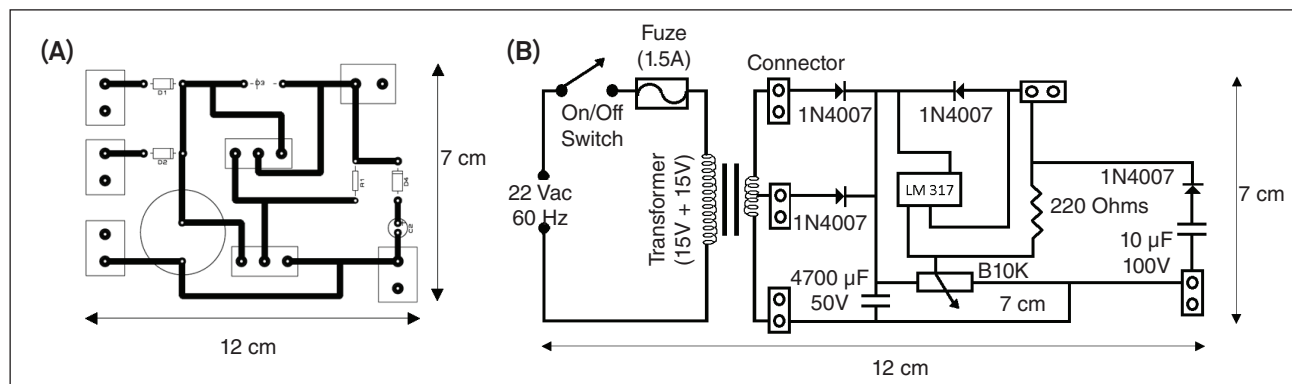


Figure 4: (A) Electrical circuit projected with Proteus Ares software and (B) electrical circuit.

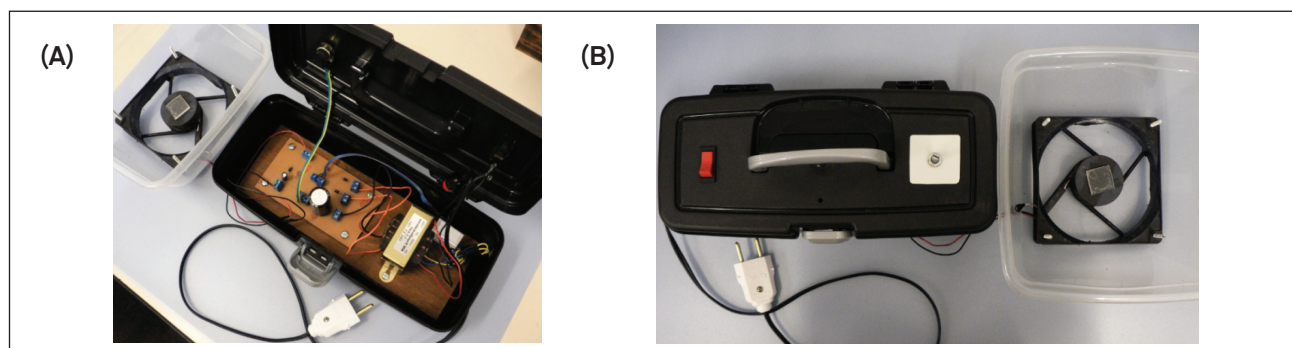


Figure 5: Complete spinner apparatus.

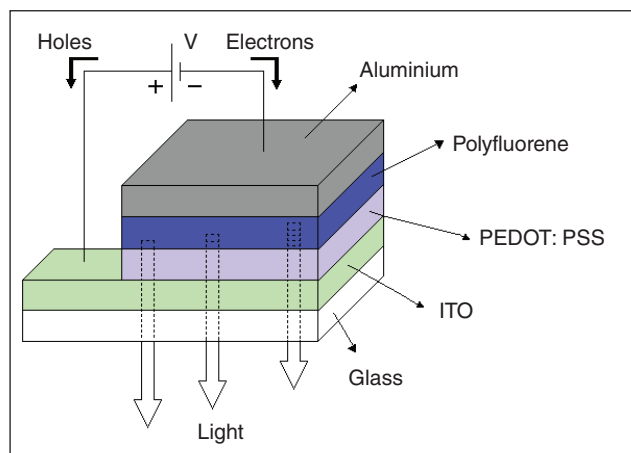


Figure 6: Structure of OLED devices assembled.

## RESULTS

The large fans, A, B and Q were investigated applying voltage (V) using the commercial power supply at: 1.5, 3.0, 4.5, 6.0, 7.5, 9.0 and 12.0 volts to obtain the rotation speed (rpm). In this interval voltage, the A and B motors showed similar results presenting below 4000 rpm, as reported by literature<sup>25-27</sup>. The Q motor presented higher values of speed in the same interval of different voltages and for this motive, it was abandoned.

Figure 7 shows the speed  $\times$  nominal voltage for fans A, B, and Q.

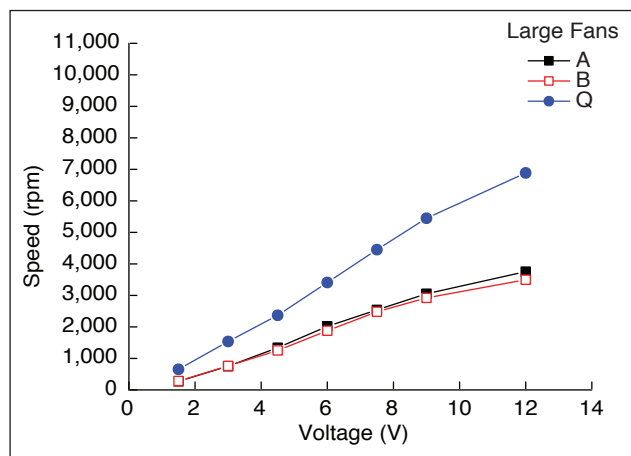


Figure 7: Speed  $\times$  nominal voltage for fans: A, B, and Q.

Figure 8 shows the performance of  $8.0 \times 8.0$  cm for little fans (C, D, E, G, H, I, and P).

In this case, fans I and P presented most usual speed range in the assembly of OLED, while the fans C, D, E, G, and H presented very high values of speed, then they were discarded to be used as spinner.

Then a comparison between little fans (I and P) and large fans (A and B) was carried out using the variable power supply mounted in the laboratory. Approximately 50 measurements were performed for each fan. Figure 9 shows the results of speed  $\times$  voltage for fans A, B, I and P.

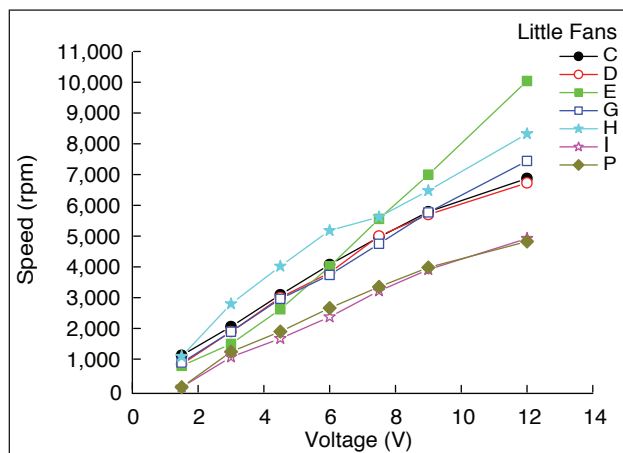


Figure 8: Speed  $\times$  nominal voltage for fans: C, D, E, G, H, I, and P.

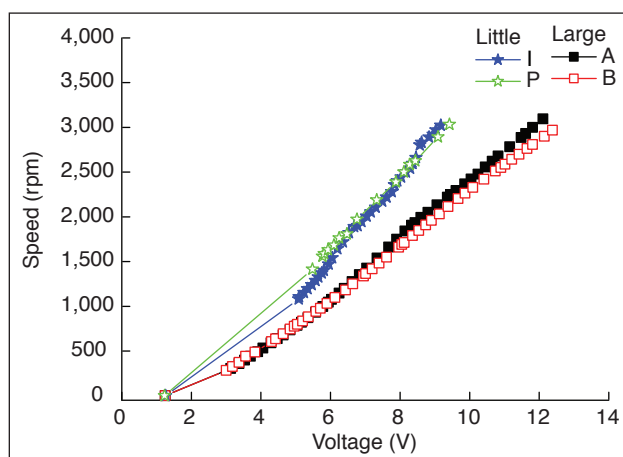


Figure 9: Speed  $\times$  voltage for fans: A, B, I, and P.

In the range from 1000 to 4000 rpm, fans A and B respond to  $\approx 3$  V stimulus, while I and P start responding only at higher applied voltage  $\approx 5$  V. However, if only the range from 1500 to 3000 rpm is considered for the deposition of thin films for OLED devices assembly, there is no significant difference.

Fans A and B presented smaller angular coefficient which makes the voltage setting with the potentiometer easier because the speed is less sensitive to voltage variation compared to fans I and P.

Another relevant fact is that fans I and P presented more vibration, this instability may cause films to have non uniform thickness.

In Fig. 10 it is observed that fan B presented the highest electrical resistance, while fan A showed the lowest for most of the applied voltage. A possible explanation for this behavior can be given by the fact that all fans tested came from obsolete computers and no information about the lifetime conditions is available.

The correlation speed  $\times$  electrical current is shown in Fig. 11. It revealed that the fan B reached the highest speed with the lowest increase of electrical current. This result was not expected, since fan A presented the electrical current increasing in a steeper trend with the applied voltage (Fig. 10), compared to fan B. It's clear that

the fans I and P presented poor results with unstable curves in the speed caused by variation of the electrical current.

On the other hand, it was difficult to determine which fan A or B is better, because both presented performance curves indicating good stability.

Fan A showed higher electrical current with the applied voltage (larger angular coefficient), is more responsive and would probably be chosen to the spinner apparatus. For a more clear interpretation, the derivatives of the speed  $\times$  voltage curves were obtained in the Fig. 12.

These results help finding the fan that presented lowest variation of speed with the applied voltage.

In addition, derivative  $\times$  voltage applied for fans A and B shown low variation. This analysis is an important characteristic for thin films deposition as increasing or decreasing voltage before setting will not affect the thickness, it means that when a specific voltage is applied it will yield the same speed even if a higher or lower voltage had been used previously. Figures 13 and 14 show the voltage applied (from 0 V to 12 V, and also from 12 V to 0 V)  $\times$  speed rotation (rpm) for fans A and B, respectively.

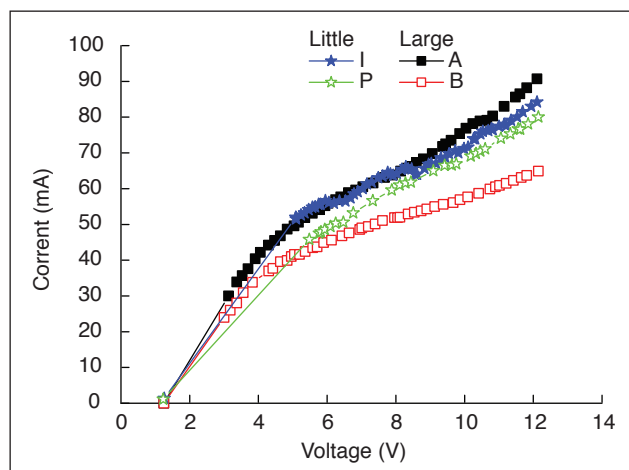


Figure 10: Electrical current  $\times$  voltage for fans: A, B, I, and P obtained with variable power supply.

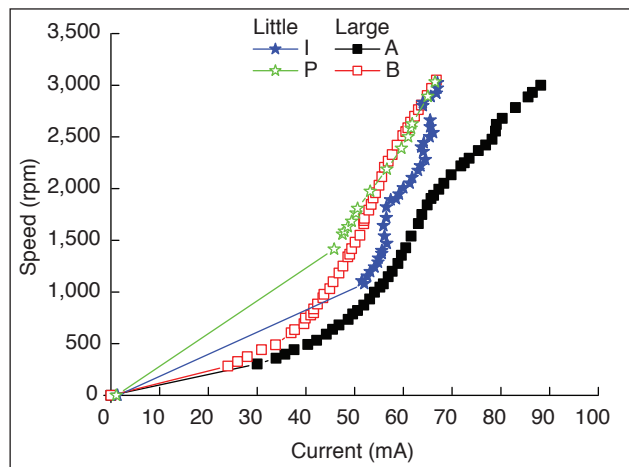


Figure 11: Speed  $\times$  electrical current for fans: A, B, I, and P obtained with variable power supply.

Fans A and B have shown similar behavior in Figs. 13 and 14, however fan A seemed to be a better choice as its current response to applied voltage (Fig. 10) is comparatively steeper. Therefore it was selected together with the variable power supply to assembly the spinner apparatus.

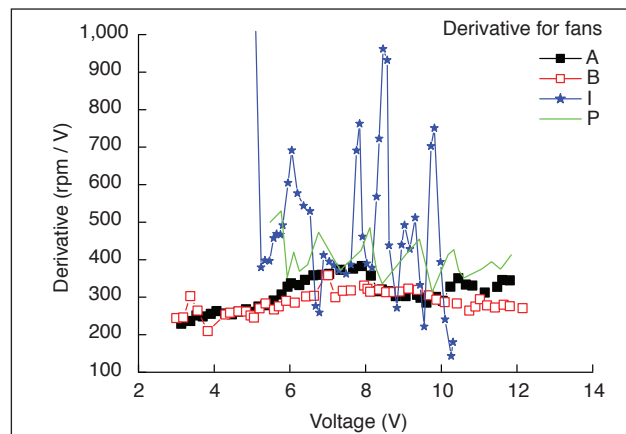


Figure 12: Derivate  $\times$  voltage for fans: A, B, I, and P obtained with the variable power supply.

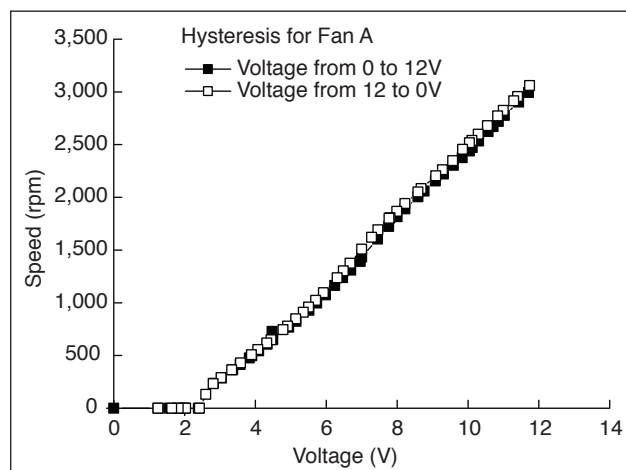


Figure 13: Speed  $\times$  voltage for fan A obtained with variable power supply.

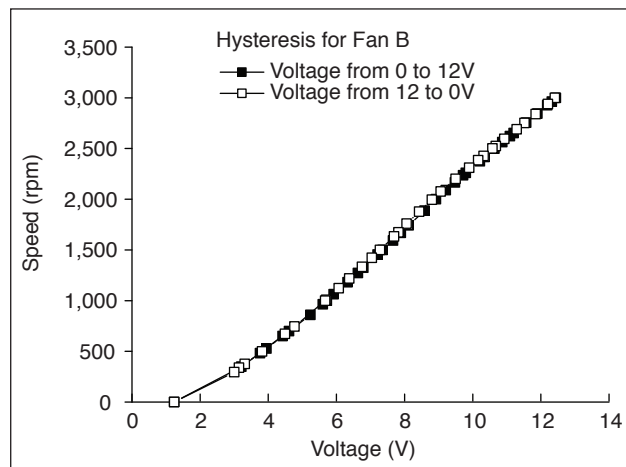


Figure 14: Speed  $\times$  voltage for fan B obtained with variable power supply.

Then photoresist on the ITO film was deposited using four different rotations (Table 3). Three measurements at different points were carried out for each sample. The fan A showed good results with low variation on the standard deviation of the thicknesses for polymeric films produced.

**Table 3:** Thicknesses of photoresist films measured by profilometry.

Sample	Speed (rpm)	Thickness ( $\mu\text{m}$ ) $\pm$ Standard deviation
1	1000	4.89 $\pm$ 0.09
2	2000	3.45 $\pm$ 0.08
3	3000	2.80 $\pm$ 0.11
4	4000	2.37 $\pm$ 0.04

The spinner apparatus with fan A was used to assembly three OLEDs with 2000 and 3000 rpm and I-V curves were obtained for each device tested. Figure 15 shows I-V curves for OLED mounted with 2000 rpm and Fig. 16 for OLEDs

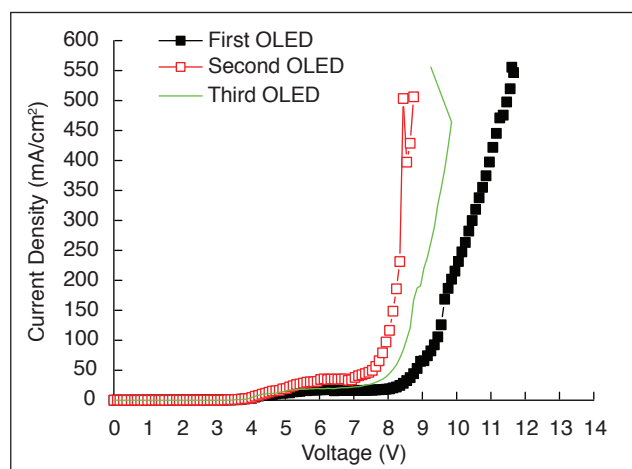


**Figure 15:** Current density  $\times$  voltage for OLED device deposited at 2000 rpm with variable power supply.

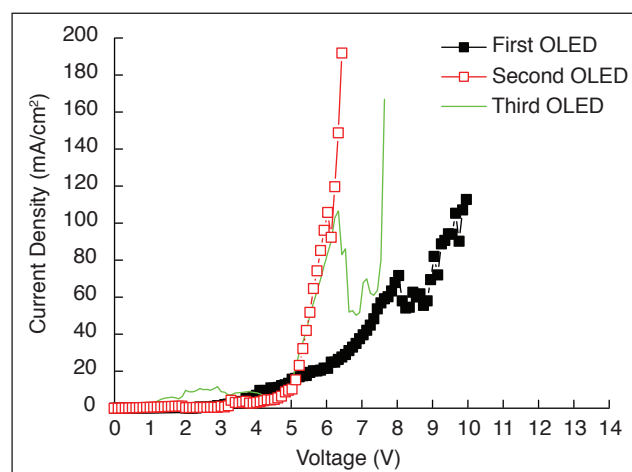


**Figure 16:** Current density  $\times$  voltage for OLED device deposited at 3000 rpm with variable power supply.

mounted with 3000 rpm. The highest electrical current density with range of threshold voltage from 8 to 9 V (obtained by imaginary tangent line to voltage axis) was found for devices of which layers deposited at 2000 rpm (Fig. 15).

These devices presented also similar aspects of diode curves. In comparison, the devices prepared at 3000 rpm (Fig. 16) showed lowest current density and some variations in the curves were also observed. In the work of Albano de Almeida OLEDs were mounted with the same structure and spinner apparatus at 3000 rpm for all layers, but the results of I-V curves revealed also poor performance in devices with highest voltage threshold and lowest electrical current<sup>28</sup>.

## CONCLUSION

The assembly of compact and low cost spinner was possible to accomplish from a power supply fan. Fans of different sizes used in microcomputers connected to a multi-step-power-supply to control it were used to test spinner configurations and performances. Later, a variable power supply was also assembled in order to achieve higher voltage resolution. In the final tests, the fans named A and B were chosen based on the following criteria: (a) contribution to the compactness of the spinner, facilitation handling in a glove box system for assembly of OLED devices; (b) amplitude of adjustable speeds, suitable to work from 1000 to 3000 rpm, used in the assembly of OLED devices; (c) stability of the speed with variation of the applied voltage (as shown by the derivative curve of speed in function of voltage). It is very important that the specific voltage applied to the spinner does not cause variations in the rotation speed to avoid non-uniformity and assure flatness in the final thickness of the thin film and (d) absence of vibration observed during the spin-coating process to preserve the good homogeneity of the polymeric layers. The apparatus spinner with fan A was used to build OLED devices and the polymeric layers were deposited at 2000 and 3000 rpm to assembly the structure: glass/ITO/PEDOT:PSS/Polyfluorene (PFpf)/Al revealing blue light emission. The OLED device prepared at 2000 rpm presented better results with highest current density and similar aspect of diode curve.

## ACKNOWLEDGEMENTS

The authors are grateful to the financial support from the Brazilian agencies: CAPES (Coordenação de Aperfeiçoamento de Pessoal de Nível Superior), CNPq (Conselho Nacional de Desenvolvimento Científico e Tecnológico) and FAPESP (Fundação de Amparo à Pesquisa do Estado de São Paulo).

They also thank Escola Politécnica da Universidade de São Paulo for providing installations and equipment.

## REFERENCES

- Romero-Servin S, Lozano-Hernández LA, Maldonado JL, Carriles R, Ramos-Ortiz G, Pérez-Gutiérrez E, et al. Light emission properties of a cross-conjugated fluorene polymer: demonstration of its use in electro-luminescence and lasing devices. *Polymers*. 2016;8(2):43-54. Available from: <https://doi.org/10.3390/polym8020043>
- Juhasz P, Nevrela J, Micjan M, Novota M, Uhrík J, Stuchlikova L, et al. Charge injection and transport properties of an organic light-emitting diode. *Beil J Nanotech*. 2016;7:47-52. Available from: <http://doi.org/10.3762/bjnano.7.5>
- MacIsaac D, Kanner G, Anderson G. Basic physics of the incandescent lamp (lightbulb). *The Phys Teach*. 1999;37(9):520-525. Available from: <https://doi.org/10.1119/1.880392>
- Philips OLED Works Naturally Illuminating, Brite 2 FL300 Family – Two shapes in warm white and neutral white; 2016.
- Roszbach S. OLED technology: challenges and new opportunities. Brabant: OSRAM 2013.
- Komoda T, Tsuji H, Ito N, Nishimori T, Ide N. High quality white OLEDs and resource saving fabrication process for lighting fabrication. *Soc Info Disp*. 2010;41(1):993-996. Available from: <https://doi.org/10.1889/1.3500653>
- Cooper EA, Jiang H, Vildavski V, Farrell JE, Norcia AM. Assessment of OLED displays for vision research. *J Vision*. 2013;13(12):16. Available from: <http://doi.org/10.1167/13.12.16>
- Correia FC. Síntese e caracterização de polímeros contendo 9,9 diocetilfluoreno e 8-octilquinolina para utilização como camada emissora de PLEDs [Doctoral Thesis]. São Paulo: Escola Politécnica da Universidade de São Paulo; 2013.
- Gaj MP, Fuentes-Hernandez C, Zhang Y, Marder SR, Kippelen B. Highly efficient organic light-emitting diodes from thermally activated delayed fluorescence using a sulfone-carbazole host material. *Organic Elect*. 2015;16:109-112. Available from: <https://doi.org/10.1016/j.orgel.2014.10.049>
- Bansal AK, Antolini F, Zhang S, Stroea L, Ortolani L, Lanzi M, et al. Highly luminescent colloidal CdS quantum dots with efficient near infrared electroluminescence in light-emitting diodes. *J Phys Chem C*. 2016;120:1871-1880. Available from: <http://doi.org/10.1021/acs.jpcc.5b09109>
- Ho S, Liu S, Chen Y, So F. Review of recent progress in multilayer solution-processed organic light-emitting diodes. *J of Photon for Energy*. 2015;5:057611. Available from: <https://doi.org/10.1117/1.JPE.5.057611>
- Santos ER, Wang SH, Correia FC, Costa IR, Sonnenberg V, Burini Jr EC, et al. Influência de diferentes solventes utilizados na deposição de filmes de poli(9-vinilcarbazol) em dispositivos OLEDs. *Quím Nova*. 2014;37(1):1-5. Available from: <http://dx.doi.org/10.1590/S0100-40422014000100001>
- Liu Y-S, Feng J, Ou X-L, Cui H-F, Xu M, Sun H-B. Ultrasmooth, highly conductive and transparent PEDOT:PSS/silver nanowire composite electrode for flexible organic light-emitting devices. *Organ Elec*. 2016;31:247-252. Available from: <https://doi.org/10.1016/j.orgel.2016.01.014>
- Zhu F. OLED activity and technology development. In: *Symposium on Sustain Driven Innovative Technologies*; Hong Kong; 2009.
- Hung W-Y, Chiang P-Y, Lin S-W, Tang W-C, Chen Y-T, Liu S-H, et al. Balance the carrier mobility to achieve high performance exciplex OLED using a triazine-based acceptor. *ACS Appl Mater Interf*. 2016;8(7):4811-4818. Available from: <http://doi.org/10.1021/acsami.5b11895>
- Tyona MD. A comprehensive study of spin coating as a thin film deposition technique and spin coating equipment. *Adv Mater Res*. 2013;2(4):181-193. Available from: <http://doi.org/10.12989/amr.2013.2.4.181>
- Bianchi RF, Panssiera MF, Lima JPH, Yagura L, Andrade AM, Faria RM. Spin coater based on brushless dc motor of hard disk drivers. *Prog Org Coat*. 2006;57(1):33-36. Available from: <https://doi.org/10.1016/j.porgcoat.2006.05.004>
- Emslie AG, Bonner FT, Peck LG. Flow of a viscous fluid on a rotating disk. *J Appl Phys*. 1958;29(5):858-862. Available from: <https://doi.org/10.1063/1.1723300>
- Meyerhofer D. Characteristics of resist films produced by spinning. *J Appl Phys*. 1978;49(7):3993-3997. Available from: <https://doi.org/10.1063/1.325357>
- Sahu N, Parija B, Panigrahi S. Fundamental understanding and modeling of spin coating process: a review. *Indian J Phys*. 2009;83(4):493-502. Available from: <https://doi.org/10.1007/s12648-009-0009-z>
- Santos ER, Correia FC, Burini Jr EC, Onmori RK, Fonseca FJ, Andrade AM, et al. Influence of the transparent conductive oxides on the P-OLEDs behavior. *ECS Trans*. 2012;49(1):347-354. Available from: <http://doi.org/10.1149/04901.0347ecst>
- Santos ER, Moraes JIB, Sonnenberg V, Onmori RK, Takimoto HG, Burini Jr EC, et al. Improvements the processes steps for assembly of OLEDs devices. In: *13º Congresso Brasileiro de Polímeros*; Natal; 2015.
- Takimoto HG. Estudo de polifluorenos como camada emissora de dispositivos eletroluminescentes eficientes [Master's Dissertation]. São Paulo: Escola Politécnica da Universidade de São Paulo; 2013.
- Almeida A. Estudo de encapsulamento em dispositivos OLEDs [Final Coursework]. São Paulo: Faculdade de Tecnologia de São Paulo; 2016.
- Siahjani S, White M, Sariciftci NS, Erten-Ela S. Fabrication and characterization of green light emitting diode. *Turk J Phys*. 2014;38:509-515. Available from: <http://doi.org/10.3906/fiz-1405-9>
- Lee D-H, Choi J, Chae H, Chung C-H, Cho SM. Single-layer organic-light-emitting devices fabricated by screen printing method. *Korean J Chem Eng*. 2008;25(1):176-180. Available from: <https://doi.org/10.1007/s11814-008-0032-3>
- Jou J-H, Su Y-T, Liu S-H, He Z-K, Sahoo S, Yu H-H, et al. Wet-process feasible candlelight OLED. *J Mater Chem C*. 2016;4:6070-6077. Available from: <http://doi.org/10.1039/C6TC01968D>
- Almeida A, Sonnenberg V, Silva ANR, Zambom LS, Burini EC, Takimoto HG, Hui WS, Santos ER. Estudo da Degradação de Dispositivos OLEDs. In: *Resumos do 18º Simpósio de Iniciação Científica e Tecnológica*; São Paulo: FATEC; 2016.